Electromagnetic Transitions for the Photodisintegration of the Deuteron

MASAHIKO MATSUMOTO*
Theoretical Physics Institute, University of Alberta, Edmonton, Canada
(Received 20 April 1962; revised manuscript received 25 June 1962)

Over-all electromagnetic transitions for the photodisintegration of the deuteron are examined in the energy range 162 to 833 MeV. The virtual meson exchange interaction is not considered. The electromagnetic interactions are treated without any series expansion. Therefore, all multipole transitions and their retardations are completely taken into account in the calculations.

The pion-theoretical deuteron wave function and plane waves are used for the initial and final states, neglecting the effects of the hard core in the nucleon-nucleon potential. It is then shown that the angular dependence of those terms which are simply isotropic in the electric dipole approximation is given approximately by the isotropic part in the electric dipole transition, plus a cosine curve due to the overlap effects of the higher multipole transitions, as well as overlap effects due to all retardations. The terms which reduce to the anisotropic terms in the electric dipole approximation give angular distributions which are shifted forward from $\sin^2\theta$ but which tend to flatten out with increasing energy. The separate retardation effects due to the dipole and other multipole terms cannot be distinguished in the present calculation.

For some reason the total cross sections seem to fit the experimental data fairly well at energies higher than 400 MeV when only the electric transitions are taken into account. However, the total cross sections including magnetic transitions are about four times the experimental data at 800 MeV. The contribution of the magnetic transitions to the cross sections does not decrease as much with energy as does the contribution due to the electric transitions and remains relatively large at high energy. The effect of disregarding the hard core is large for the spin magnetic transitions.

I. INTRODUCTION

FOR the photodisintegration of the deuteron in the energy range below 100 MeV,[1–7] the experimental data have been satisfactorily reproduced within the framework of the present information concerning nuclear forces and radiative interactions, without renouncing the Siegert theorem for the electric transitions. A ground-state deuteron wave function, which contains a somewhat large percentage of d state (6.7%), and a final-state wave function consistent with nucleon scattering, have formed the basis of calculations of the transition probabilities; for example, a strong positive tensor potential in triplet odd states and inclusion of the triplet F-state contribution in final states, satisfactorily account for the large isotropic part in the observed angular distributions.

Concerning the radiative interaction, it appears that one can regard the entire effect as essentially a classical one with no meson contributions of importance. The main features of the reaction can be described through electric dipole and electric quadrupole transitions; however, other contributions, such as the magnetic dipole and magnetic quadrupole transitions, as well as the retardation[8] effects for each multipole transition, must be taken into account. Extensive investigations in this field for the magnetic dipole and quadrupole transitions have been worked out by Breit and his collaborators,[4] and by Kramer and Werntz.[7] These authors have shown that these effects are smaller than 5% of the electric dipole transition cross section; however, the interference terms between the electric dipole and the magnetic transitions to the triplet final states account for the large asymmetries of the angular distributions.

On the other hand, the relative smallness of the retardation effect has been reported by Nicholson and Brown,[3] and also by Kramer and Werntz[9] in a more detailed manner. The latter used a Hulthén wave function for the deuteron with 4% d-state probability, and a final-state wave function calculated from the Signell and Marshak potential.[10] The difference between the electric dipole interaction including the retardation and the usual one becomes significant at a distance of about one-fourth of the photon wavelength. Thus, the retardation contributions may be expected to be effective at energies such that one-fourth of the photon wavelength is smaller than the nuclear force range. The cross section due to the electric transition in the range 80 to 300 MeV has been calculated by the author, taking into account all retardations and all multipole transitions[11]; it was

* On leave from the Shiga University, Otsu, Japan.
[1] J. Iwadare, S. Otsuki, R. Tamagaki, and W. Watari, Progr. Theoret. Phys. (Kyoto) **16**, 658 (1956).
[2] J. J. de Swart and R. E. Marshak, Phys. Rev. **111**, 272 (1958).
[3] A. F. Nicholson and G. E. Brown, Proc. Phys. Soc. (London) **73**, 221 (1959).
[4] W. Zernik, M. L. Rustgi, and G. Breit, Phys. Rev. **114**, 1358 (1959); M. L. Rustgi, W. Zernik, G. Breit, and D. J. Andrews, *ibid.* **120**, 1881 (1960); W. Zickendraht, D. J. Andrews, M. L. Rustgi, W. Zernik, A. J. Torruella, and G. Breit, *ibid.* **124**, 1538 (1961); W. Zickendraht, D. J. Andrews, and M. L. Rustgi, Phys. Rev. Letters **7**, 252 (1961).
[5] J. J. de Swart and R. E. Marshak, Physica **25**, 1001 (1959).
[6] J. Iwadare and M. Matsumoto, Progr. Theoret. Phys. (Kyoto) **24**, 797 (1960).
[7] G. Kramer and C. Werntz, Nucl. Phys. **15**, 60 (1960); Phys. Rev. **119**, 1627 (1960).
[8] We use the term retardation here in a special sense, viz., to describe the difference in an expansion of the interaction in powers of the wave vector and in spherical harmonics.
[9] G. Kramer and C. Werntz have shown only 4% d-state probability for the deuteron wave function is sufficient to give agreement with experiment. This circumstance is due to the large interference between the electric dipole and magnetic quadrupole transitions.
[10] P. S. Signell and R. E. Marshak, Phys. Rev. **109**, 1229 (1958).
[11] M. Matsumoto, Progr. Theoret. Phys. (Kyoto) **23**, 597 (1960).

shown in this work that rather remarkable effects do appear in the angular distributions. It might be noted that even for electric dipole transitions only, the retardation effect has been reported to be large.[12] These conclusions, however, differ from those of Nicholson and Brown, and of Kramer and Werntz.

The interference of the magnetic triplet transition with the electric transitions makes a particularly large asymmetry in the angular distributions, as has been pointed out by Breit *et al.*[4] The purpose of the present paper is to complete the calculations of the electric, magnetic triplet, and magnetic spin-flip transitions, including all multipole transitions and their retardations, and then to clarify their relative effects in the energy region 162- to 800-MeV incident photon energy. The experimental data[13] at energies around the virtual meson threshold show effects of overlap from the contributions of the virtual mesons and the electromagnetic interactions. The virtual meson effects should, in principle, provide a check on the internal consistency of the meson theory[14]; unfortunately, this energy region is not suitable for the test since the exact cross sections for the pure electromagnetic interactions would have to be known. The comparison between experimental data and theoretical results in this energy region is also not very significant, since the phenomenological potential used is known to give very poor values for the scattering of nucleons. The final-state continuum radial wave functions consistent with nucleon scattering data are unknown at the present stage. The plane wave approximation (no interaction in the final states) is generally used, but without complete justification, in the energy region higher than the virtual meson threshold. Our calculations are based on the expression for the interaction between the deuteron and the photon field which was derived by Foldy.[15]

The excitation curve for the photodisintegration of the deuteron, excluding pion emission, was measured by Myers *et al.*[16] The experimental results show that the total cross sections decrease monotonically from 7.0 ± 1.0 μb at 508 MeV to 1.0 ± 1.0 μb at 913 MeV and give no indication of a second resonance due to virtual mesons. On the other hand, these results compare very well with the calculations of the present paper. We take this to be good evidence for the significant role played by the electromagnetic retardations.

In Sec. II, the electric transition, the magnetic spin-flip and triplet transitions, and the transitions due to the convection current interaction are calculated in the same fashion as in reference 11 taking into account relativistic effects in the energy calculation. In Sec. III, the results of all calculations are shown, and the multipole effects and their retardations are compared with the dipole transition. Discussion of the results and concluding remarks are given in Sec. IV.

II. CALCULATION OF TRANSITION MATRIX

The electric and magnetic transitions from the deuteron ground state ψ_g to the final state ψ_f are specified by selection rules. The 2^L-pole transition has parity change $(-)^L$ for electric and $(-)^{L+1}$ for magnetic transitions. These selection rules for multipole transitions are satisfied automatically when the electromagnetic interaction is used without multipole expansion. The expression for the complete interaction including all multipoles has the disadvantage of being rather cumbersome. It is usual to reduce it to the corresponding dipole terms for comparison.

In order to include all possible transitions, we use a plane wave for the final-state wave function. We then have for the triplet and singlet final-state wave functions, respectively,

$$\psi_f{}^t=(1/\sqrt{2})[\pi_1\nu_2\exp(i\mathbf{k}\cdot\mathbf{x})-\pi_2\nu_1\exp(-i\mathbf{k}\cdot\mathbf{x})]\chi^t, \quad (1)$$

$$\psi_f{}^s=(1/\sqrt{2})[\pi_1\nu_2\exp(i\mathbf{k}\cdot\mathbf{x})+\pi_2\nu_1\exp(-i\mathbf{k}\cdot\mathbf{x})]\chi^s, \quad (2)$$

where $\mathbf{x}=\mathbf{x}_p-\mathbf{x}_n$ is the relative coordinate of the proton and the neutron measured in units of the π-meson Compton wavelength $\hbar/\mu c$. π_i and ν_i are the isotopic spin functions with π_i corresponding to ith particle in a proton state and ν_i corresponding to the ith particle in a neutron state. $\chi^{t(s)}$ is the final-state spin wave function for the triplet (singlet) state.

We adopt the pion theoretical deuteron wave function[17] for the initial-state wave function. This wave function is very similar to that obtained by Gartenhaus[18] for his potential. Both give the observed values of deuteron parameters, binding energy, quadrupole moment, and effective range. Moreover, they are consistent with the deuteron photodisintegration results below 100 MeV. The expression for the wave function is

$$\psi_u=\psi_d(x)\chi^t(\pi_1\nu_2-\nu_1\pi_2)/\sqrt{2},$$

with

$$\psi_d(x)=\frac{1}{(4\pi)^{1/2}}\left[u(x)/x+\frac{1}{\sqrt{8}}S_{12}w(x)/x\right], \quad (3)$$

where S_{12} is the tensor operator, and $u(x)$ and $w(x)$ are normalized in the sense $\int\{[u(x)]^2+[w(x)]^2\}dx=1$. For

[12] S. H. Hsieh, Progr. Theoret. Phys. (Kyoto) **21**, 585 (1959).
[13] C. Allen, Jr., Phys. Rev. **98**, 705 (1955); J. C. Keck and A. V. Tollestrup, *ibid.* **101**, 360 (1956); E. A. Whalin, B. D. Schriever, and A. O. Hanson, *ibid.* **101**, 377 (1956).
[14] J. Fujimura and S. Nagahara, Progr. Theoret. Phys. (Kyoto) **9**, 132 (1953); F. Zachariasen, Phys. Rev. **101**, 371 (1956); R. Suzuki, Progr. Theoret. Phys. (Kyoto) **15**, 366 (1956); L. D. Perlstein and A. Klein, Phys. Rev. **118**, 193 (1960); T. Akiba, Progr. Theoret. Phys. (Kyoto) **24**, 370 (1960).
[15] J. M. Berger, Phys. Rev. **94**, 1698 (1954); L. L. Foldy, *ibid.* **92**, 178 (1953).
[16] H. Myers, R. Gomes, D. Guinier, and A. V. Tollestrup, Phys. Rev. **121**, 630 (1961).
[17] J. Iwadare, S. Otsuki, R. Tamagaki, and W. Watari, Progr. Theoret. Phys. (Kyoto) **16**, 455 (1956).
[18] S. Gartenhaus, Phys. Rev. **100**, 900 (1955); J. Gammel and R. Thaler, *ibid.* **107**, 291 (1957).

simplicity in calculations, we use the following analytical form to approximate the pion theoretical wave function:

$$u(x)=1.039[\exp(-0.328x)-\exp(-1.972x)], \quad (4)$$

$$w(x)=0.111\exp(-0.4x)+0.656\exp(-1.0x) -0.767\exp(-2.0x). \quad (5)$$

The wave functions (4) and (5) fit the pion theoretical or Gartenhaus wave functions in the outer region and reproduce the following deuteron parameters:

$$Q=2.6\times10^{-27}\ \text{cm}^2,$$
$$d\text{-state probability}=0.07,$$
$$^3r_t=1.7\times10^{-13}\ \text{cm}.$$

That these approximate wave functions $u(x)$ and $w(x)$ start from the origin in a different manner than the theoretical deuteron wave function arises from the fact that effects of the hard core of the potential have been neglected in the initial-state wave function. The shape of the inner wave function[18] is not very reliable, reflecting the lack of our knowledge about the inner potential at the present time; fortunately, it does not affect the electric transition matrix elements significantly. The discussions about effects of the hard core is later resumed in Sec. IV.

1. Electric Transitions

The electric transitions, which lead to the main features of the angular distributions, have been considered in reference 11. Here we use the same interaction; then the matrix element of the electric transition[15,19] from the deuteron ground state to the triplet final state (1) is

$$\mathrm{El}=\left\langle\chi^t\middle|\int_0^1 ds\int \exp(-i\mathbf{k}\cdot\mathbf{x})(\mathbf{e}\cdot\mathbf{x}/2) \times\exp(is\boldsymbol{\kappa}\cdot\mathbf{x}/2)\psi_d(x)d\mathbf{x}\middle|\chi^t\right\rangle, \quad (6)$$

where $\boldsymbol{\kappa}$ is the wave vector of the incident photon, $\mathbf{e}$ is the photon polarization vector, and $\mathbf{k}$ is the wave number of the outgoing particle. s is a parameter. If one simply puts $s=0$ or, equivalently, takes the first term in a power series expansion of the interaction in Eq. (6), then one gets the usual expression $\mathbf{e}\cdot\mathbf{x}/2$ for the electric dipole interaction. When the interaction term in Eq. (6) is expanded in terms of the angular momenta, then $j_0(s\kappa x/2)$ gives the first term. The effect of the retardation with this form was examined by Nicholson and Brown.[3] Here we calculate the complete matrix elements El without using any expansion for the retardation factors.

[19] R. G. Sachs, *Nuclear Theory* (Addison-Wesley Publishing Company, Reading, Massachusetts, 1953), p. 238.

2. Magnetic Transitions

The spin-flip magnetic transitions have the next largest effect to the electric transitions. The magnetic triplet transitions give a very small cross section, but these transitions interfere with the electric transitions and are expected to push the angular distributions significantly forward despite little variation in the total cross sections.

The transition matrix elements for the spin flip magnetic transition may be written

$$\mathrm{Ms}=\left\langle\chi^s\middle|\frac{\mu}{2M}(\boldsymbol{\sigma}_1-\boldsymbol{\sigma}_2)\cdot(\mathbf{e}'/2) \times\int d\mathbf{x}[\mu_p\exp(i\mathbf{K}_1\cdot\mathbf{x})-\mu_n\exp(i\mathbf{K}_2\cdot\mathbf{x})]\psi_d(x)\middle|\chi^t\right\rangle; \quad (7)$$

while the magnetic triplet transition may be written

$$\mathrm{Mt}=\left\langle\chi^t\middle|\frac{\mu}{2M}(\boldsymbol{\sigma}_1+\boldsymbol{\sigma}_2)\cdot(\mathbf{e}'/2) \times\int d\mathbf{x}[\mu_p\exp(i\mathbf{K}_1\cdot\mathbf{x})+\mu_n\exp(i\mathbf{K}_2\cdot\mathbf{x})]\psi_d x)\middle|\chi^t\right\rangle. \quad (8)$$

Here $\mathbf{K}_1=(\boldsymbol{\kappa}/2)-\mathbf{k}$, $\mathbf{K}_2=(\boldsymbol{\kappa}/2)+\mathbf{k}$, $\mathbf{e}'=(\boldsymbol{\kappa}\times\mathbf{e})/|\kappa|$, and $\boldsymbol{\mu}_p$, $\boldsymbol{\mu}_n$, are the magnetic moments of proton and neutron, respectively, expressed in nuclear magnetons. $\boldsymbol{\sigma}_i$ is the spin operator associated with the ith nucleon.

In the magnetic dipole transition, the photon momentum is not involved in the interaction term (i.e., $\kappa=0$). Therefore, the interaction term in Eq. (7) reduces to the magnetic spin-flip interaction $\frac{1}{2}(\boldsymbol{\sigma}_1-\boldsymbol{\sigma}_2)\cdot(\boldsymbol{\mu}_p-\boldsymbol{\mu}_n)$. In the same way, Eq. (8) reduces to the interaction $\frac{1}{2}(\boldsymbol{\sigma}_1+\boldsymbol{\sigma}_2)\cdot(\boldsymbol{\mu}_p+\boldsymbol{\mu}_n)$ which gives rise to the magnetic transition to the triplet final state in the dipole case.

For the magnetic transition due to the convection current, the transition matrix element may be written

$$\mathrm{Mc}=\left\langle\chi^t\middle|\frac{1}{2Mc}\int_0^1 sds\int \exp(-i\mathbf{k}\cdot\mathbf{x})[\mathbf{x}\times\mathbf{p}]\cdot\mathbf{e}' \times\exp(is\boldsymbol{\kappa}\cdot\mathbf{x}/2)\psi_d(x)d\mathbf{x}\middle|\chi^t\right\rangle, \quad (9)$$

where $\mathbf{p}$ is the momentum conjugate to $\mathbf{x}$.

III RESULTS

The calculations of the previous section were performed at seven angles for each of the photon energies 162, 411, 510, 715, and 833 MeV, in the lab system. In the following, we look at the differential cross sections,

the total cross sections, the multipole effects, and the interference effects between the electric and the magnetic transitions to the triplet final states.

1. Electric Transition

The differential cross section for the electric transition is calculated to be

$$d\sigma(\mathrm{El})/d\Omega = B(k)k^2\{16(Y'^2+Y^2\sin^2\theta)+(12X''^2+11Y^2 +3Z^2+28X'Y'+4X''Z+10YZ)\sin^2\theta +[32X'^2+4X(Z+7Y-2X'')]\sin^4\theta +4(X'Y'-X''Y+3X^2\sin^4\theta)\sin^2\theta\}, \quad (10)$$

where $B(k)=\frac{1}{12}(e^2/\hbar c)(Mc\kappa/\hbar)k^{-1}(\hbar/\mu c)^3$, and the transition amplitudes are

$$X=\int_0^1 ds\left(\frac{k}{K}\right)^3(\tfrac{3}{8})I(Fd),$$

$$X'=\int_0^1 ds\left(\frac{k^2}{K^3}\right)(\tfrac{1}{2}s\kappa-k\cos\theta)(\tfrac{3}{8})I(Fd),$$

$$X''=\int_0^1 ds\left(\frac{k}{K^3}\right)(\tfrac{1}{2}s\kappa-k\cos\theta)^2(\tfrac{3}{8})I(Fd),$$

$$Y=-\int_0^1 ds\left(\frac{k}{K}\right)\left(\frac{3}{20}\right)[I(Pd)+I(Fd)], \quad (11)$$

$$Y'=-\int_0^1 ds\left(\frac{1}{K}\right)(\tfrac{1}{2}s\kappa-k\cos\theta)\left(\frac{3}{20}\right)[I(Pd)+I(Fd)],$$

$$Z=-\int_0^1 ds\left(\frac{k}{K}\right)\left[\frac{I(Ps)}{\sqrt{2}}-\frac{I(Pd)}{4}\right],$$

and the overlap integrals are

$$I(Fd)=\int j_3(Kx)w(x)x^2dx,$$

$$I(Pd)=\int j_1(Kx)w(x)x^2dx, \quad (12)$$

$$I(Ps)=\int j_1(Kx)u(x)x^2dx.$$

Here $K^2=(\frac{1}{2}s\kappa-k\cos\theta)^2+(k\sin\theta)^2$, and $j_1(Kx)$ and $j_3(Kx)$ are the first- and third-order spherical Bessel functions.[20]

The results of the numerical calculation of Eq. (10) are shown in Fig. 1. Obviously, the forward asymmetry of the peak is due to the integration over the parameter s. The lower limit of the integration $s=0$ gives, as we can easily see from Eq. (6), the electric dipole transition. The overlap integrals $I(Fd)$, $I(Pd)$, and $I(Ps)$ in Eq. (12) then reduce to the dipole transition amplitudes corresponding to the transitions from the deuteron s or d states to final P or F states.[21] The quantities a_0, b_0, which specify the angular distribution

$$a_0+b_0\sin^2\theta,$$

and the total cross section $\sigma_T=4\pi(a_0+\frac{2}{3}b_0)$ for the dipole approximation are tabulated in Table I.

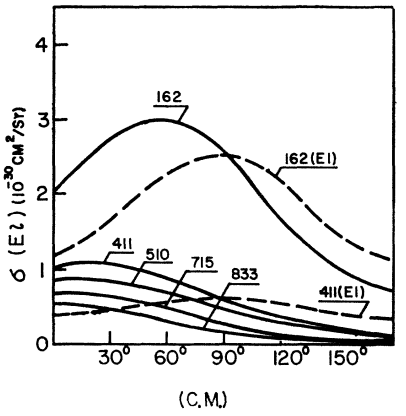

FIG. 1. Differential cross sections σ(El) for the total electric transition. The number on each curve indicates the energy (MeV) of the incident photon (lab system). The dashed curve gives the dipole approximation ($E1$).

TABLE I. The angular distribution parameters a_0, b_0 in μb/sr, and the total cross section σ_T for the electric dipole approximation.

E (MeV)	a_0	b_0	σ_T (μb)
162	1.173	1.344	26.0
411	0.408	0.275	7.45
510	0.306	0.197	5.50
715	0.203	0.127	3.60
833	0.142	0.089	2.66

In order to compare the angular distributions in Fig. 1 and those corresponding to the dipole approximation above, it is convenient to express the exact theoretical curves in Fig. 1 in the following approximate form:

$$\sigma(\mathrm{El})=a+b\sin^2\theta+c\cos\theta+d\sin^2\theta\cos\theta +e\sin^2\theta\cos^2\theta, \quad (13)$$

where a, b, c, d, and e are constants adjusted to each curve. These angular distribution parameters are shown in Table II. We can see that the main parts of a and b are obtained from the dipole transition at lower energy (e.g., 162 MeV). And these quantities do decrease with energy—relatively, a increases and b decreases with increasing energy. The interference terms due to the higher multipoles are represented by the terms involving

[20] L. I. Schiff, *Quantum Mechanics* (McGraw-Hill Book Company, New York, 1949), p. 77. J. M. Blatt and V. Weisskopf, *Theoretical Nuclear Physics* (John Wiley & Sons, Inc., New York, 1952).

[21] Exact correspondence between this limit and the exact phase-space expression is shown in reference 11.

TABLE II. The angular distribution parameters in μb/sr and the total cross sections due to all electric transitions.

E (MeV)	a	b	c	d	e	σ_T (μb)
162	1.371	1.027	0.632	1.100	0.699	26.98
411	0.614	0.007	0.415	0.176	0.179	8.06
510	0.502	−0.053	0.362	0.093	0.118	6.06
715	0.382	−0.095	0.298	0.019	0.056	4.10
833	0.306	−0.109	0.251	−0.021	0.020	2.96

c and d. Of course, the e term represents the effects of all multipoles higher than the quadrupole. From the modified expression Eq. (13) for the curves in Fig. 1, one can calculate the total cross sections easily to be of the form

$$\sigma_T=4\pi[a+(2/3)b+(2/15)e]. \tag{14}$$

The contributions of the e term to the total cross sections vary from 4.1 to 1.1% as the energy varies from 162 to 833 MeV. On the other hand, the contributions for all multipoles (including their retardations) higher than the dipole can be understood from Tables I and II; in fact, they contribute only 3.8 to 10% of the total cross section in this energy range. Here there may seem to be some contradiction with the fact that, at 162 MeV the estimated value 4.1% of the contribution of the e term to the total cross section is *larger* than the value 3.8% of whole increment to the dipole approximation due to the retardation and the multipole effects. But it should be kept in mind, that these angular distribution parameters were used only for convenience in the calculation of the total cross sections and because they provided simple analytical expressions for the calculated differential cross sections. The apparent contradiction must come from the fact that the deformations of the angular distributions correspond to marked forward shifts—i.e.,

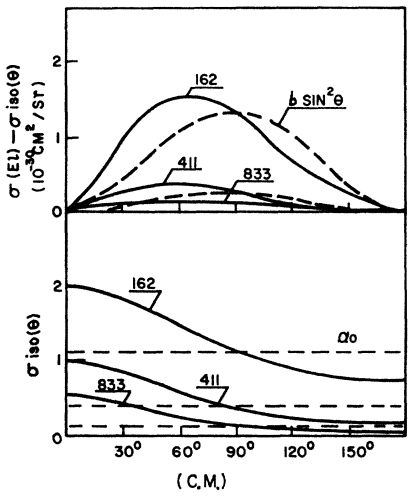

FIG. 2. Lower diagram: angular dependence of $\sigma_{iso}(\theta)$ according to Eq. (15); upper diagram: $\sigma(\mathrm{El})-\sigma_{iso}(\theta)$, that is Eq. (15) subtracted from Eq. (10). Dashed lines correspond to the values of a_0 for each energy. The number on each curve indicates the energy (MeV) of the incident photon.

to large values of c, d, and e. Naturally, the parameters a, b, c, d, and e do not have an exact correspondence with multipole transitions in so far as we do not limit the order of multipoles.

Let us now look back to Eq. (10) to see the behavior of the first term in curly brackets which reduces to a_0, and also the other terms which reduce to b_0, in the limit of the dipole approximation. Each transition amplitude depends upon K and K involves θ in such a manner that the cross sections at forward angles have larger values than at backward angles. As a result, we can understand the behavior of the term

$$\sigma_{iso}(\theta)=B(k)k^2(Y'^2+Y^2\sin^2\theta)16 \tag{15}$$

in Fig. 2, and, in particular, its marked forward shift. It seems to be approximately expressed by a_0 and a cosine term. At lower energies, for example, at 162 MeV, the value of this term at 90 deg is close to a_0 but it decreases with increasing energy. The angle corresponding to the value a_0 shifts forward in accordance with the relation $s\kappa=4k\cos\theta$ as the energy increases, as can be seen from Fig. 2.

We may say that the deviations from isotropy in Eq. (15) which vanish in the dipole approximation are due to the retardations associated with the electric dipole and electric quadrupole transitions, provided that we can neglect the effect of all multipoles higher than the electric quadrupole transition.[22] Otherwise, we must be content to say that *these deviations from isotropy are due to the higher multipoles and their retardations*, at least in so far as the present analysis is concerned. We can not separate, in our treatment, the effects of the multipoles higher than the electric quadrupole; nor can we separate the retardation effects of multipoles other than the electric dipole and the electric quadrupole.

The terms in Eq. (10) remaining after subtraction of the term (15) have the angular dependence shown in Fig. 2. The maximum value decreases and the angle of the maximum value gradually shifts with increasing energy.

2. Magnetic Spin Transitions

By estimating the order of the interactions (7) and (8), we can see that the magnetic transition amplitudes are smaller than the electric ones by about $(\mu/2M)(\mu_p-\mu_n)\sim 35\%$ for the spin flip transition (7), and about $(\mu/2M)(\mu_p+\mu_n)\sim 6.6\%$ for the spin triplet transition (8). The spin triplet transitions are probably small enough to be considered negligible; nevertheless, for our present purpose we wish to examine their behavior as a function of energy. The differential cross section is

$$\sigma(\mathrm{Ms})=B(k)k^2(\mu/2M)^2 \times[(Y_s+Z_s)^2+4X_s''(X_s''+Z_s+Y_s) +8(X_s')^2\sin^2\theta+4X_s^2\sin^4\theta] \tag{16}$$

[22] This assumption was used in reference 11.

for the spin flip transitions, and

$$\sigma(\mathrm{Mt})=B(k)k^2(\mu/2M)^2\{(Y_t+Z_t)^2+(2X_t'')^2 +[2X_t(Y_t+Z_t-2X_t'')+12(X_t')^2]\sin^2\theta +4X_t^2\sin^4\theta\} \quad (17)$$

for the spin triplet transitions, where

$$X_{s(t)}=\mu_pX_1\mp\mu_nX_2,$$
$$Y_{s(t)}=\mu_pY_1\mp\mu_nY_2,$$
$$Z_{s(t)}=\mu_pZ_1\mp\mu_nZ_2,$$
$$X_{s(t)}'=\pm\mu_pX_1(\tfrac{1}{2}\kappa-k\cos\theta)/k +\mu_nX_2(\tfrac{1}{2}\kappa+k\cos\theta)/k, \quad (18)$$

and

$$X_{s(t)}''=\mu_pX_1(\tfrac{1}{2}\kappa-k\cos\theta)^2/k^2 \mp\mu_nX_2(\tfrac{1}{2}\kappa+k\cos\theta)^2/k^2.$$

The upper sign is for the suffix s, the lower sign is for the suffix (t). The overlap integrals are given by

$$X_i=-\int j_2(K_ix)\frac{3}{\sqrt{8}}w(x)xdx\left(\frac{k}{K_i}\right)^2,$$

$$Y_i=\frac{1}{\sqrt{2}}\int[j_0(K_ix)+j_2(K_ix)]w(x)dx, \quad (19)$$

and

$$Z_i=2\int j_0(K_ix)\left[u(x)-\frac{1}{\sqrt{8}}w(x)\right]xdx, \quad (i=1,2),$$

where $j_0(K_ix)$ and $j_2(K_ix)$ are the zero-order and second-order spherical Bessel functions, respectively.[20] The transition amplitudes have been calculated separately for the contributions due to proton spin and neutron spin. Their forms, reduced to the dipole approximation, are obtained as before and they agree with the results calculated in reference 6. The results of the numerical calculations of $\sigma(\mathrm{Ms})$ show (see Fig. 3) that very little deviation from the dipole approximation occurs. The angular dependence of the overlap integrals for $i=2$ in Eq. (19) is given by replacing θ by $\pi-\theta$ in the integrals for $i=1$, because $K_1(\theta)=K_2(\pi-\theta)$. Each term in Eq. (18) is just a weighted sum of μ_p and μ_n for $i=1$ and 2, because the sign of the neutron magnetic moment is negative. Thus, the angular dependences of the integrals $i=1$ and $i=2$ compensate each other and the terms in Eqs. (18) show mild angular variations which are nearly equal to those of the dipole approximation. The strong retardation effects are therefore, not seen in the angular distributions of the spin flip magnetic transition.

On the other hand, the magnetic spin triplet transitions (see Fig. 3) show marked forward angular distributions. As we discussed before, X_s, Y_s, and Z_s do not show strong variation with angles. But in the case of X_t, Y_t, and Z_t, the signs are not the same at forward and backward angles, and the values at 90 deg are close to the values for the dipole approximation. Therefore, the cross sections for the dipole approximation in this case must be close to the minimum value of the cross section. More specifically, the retardation effects come from consideration of the momentum transfer to the outgoing nucleons. As a result, the outgoing proton and neutron do not have the same momentum in the center-of-mass system and behave differently with regard to the magnetic interactions. Thus, the retardation and multipole effects account, in general, for the major trend toward forward angular distributions, and one gets results close to the dipole approximation at 90 deg.

The percentages of the total cross sections represented by the electric dipole transitions are 27 to 92% for the $\sigma_T(\mathrm{Ms})$, 7 to 75% for the $\sigma_T(\mathrm{Mt})$. While the electric dipole cross sections decrease quickly with energy, the

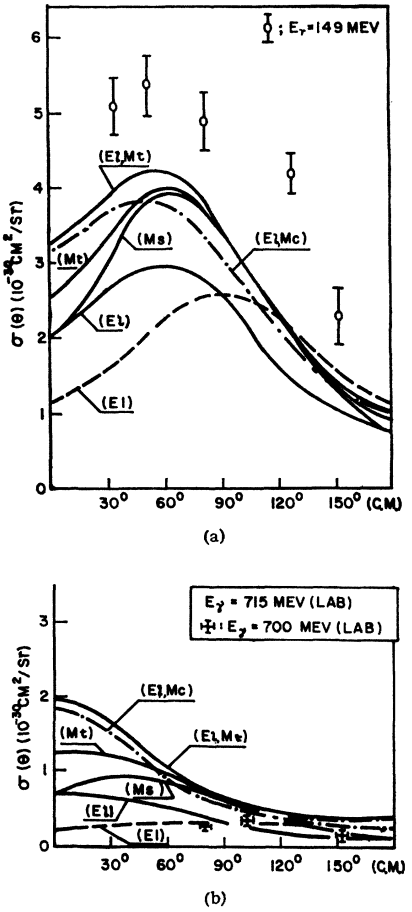

FIG. 3. Differential cross sections for the $D(\gamma,p)n$ reaction. The total electric transition cross section, the magnetic spin flip cross section, the magnetic triplet cross section, and the electric-magnetic spin triplet interference term are added up successively to give the curves marked (El), (Ms), (Mt), and (El, Mt). Finally, the electric-magnetic convection current interference term is subtracted to give the resultant curve labeled (El, Mc). The curve ($E1$) for the electric dipole approximation is given for the purpose of comparison. (A) and (B) correspond to energies 162 and 715 MeV.

cross sections of the spin magnetic transition do not change very much.

3. Magnetic Convection Current Transitions

In the matrix element for this transition, the factor $(\hbar/2Mc)(s/2)\kappa$ comes from the factor $[\mathbf{x}\times\mathbf{p}]\cdot\mathbf{e}'/2Mc$ in Eq. (9); otherwise the calculations are the same as for the electric transitions. The only essential difference is the parameter integrals have s^2ds instead of ds in Eq. (11) which makes the transition amplitudes smaller. We can expect from these considerations similar angular distributions to the angular distribution obtained for the electric transitions, but with much smaller absolute values.

The differential cross sections for these transitions vanish in the limit of the dipole approximation. There may be a good deal of interest in the interference terms between the electric and the magnetic convection current transitions.

4. Interference Terms

In the photodisintegration of the deuteron, the transitions take place between the deuteron ground state and triplet final states of the neutron-proton system except for the spin flip transition. Although transitions other than the electric transitions are small in absolute value, nevertheless, the interference terms can contribute significantly.

(A) *Interference between Electric Transitions and Magnetic Convection Transitions*

This interference is calculated by substituting the terms $X+X_c$, $Y+Y_c$, $\cdots$ for X, Y, $\cdots$ Z in Eq. (10), where X_c, X_c', $\cdots$, Z_c are the same kind of transition amplitudes as occurred in Eqs. (11), multiplied by the factor $-(\mu\kappa/2M)$; of course, the parameter integrals involve s^2ds instead of ds. The differential cross section

$$\sigma(\theta)=\sigma(\mathrm{El})+\sigma(\mathrm{El,\ Mc})+\sigma(\mathrm{Mc}) \qquad (20)$$

is shown in Fig. 3. The third term $\sigma(\mathrm{Mc})$ is negligibly small, and the interference term $\sigma(\mathrm{El,\ Mc})$ is negative so that it has the effect of decreasing the cross sections.

(B) *Interference between Electric and Magnetic Triplet Transitions*

The differential cross section for this interference term is written

$$\begin{aligned}\sigma(\mathrm{El,\ Mt})=B(k)k^2(\mu/2M)4\{&-8^{1/2}Y'X_t''+8^{1/2}YX_t'\sin^2\theta\\&+[\sqrt{2}(YX_t'+Y'X_t)\\&-8^{1/2}(X'X_t''+X''X_t')]\sin^2\theta\\&+8^{1/2}(XX_t'+X'X_t)\sin^4\theta\}.\end{aligned} \qquad (21)$$

In the dipole approximation, this term reduces simply to the term

$$c_0\cos\theta,$$

and does not contribute to the total cross sections. The value of c_0 is 0.28, 0.117, and 0.067 μb/sr at energies 162, 510, and 833 MeV, respectively. There are many interference terms left between the electric and the magnetic triplet transitions with the same parity change. They contribute positively to the cross sections and make large forward angular distributions. There is very little change in the forward differential cross sections with energy in this energy region. These interference terms are shown in Fig. 3 at energies of 162 and 715 MeV, respectively, along with the angular distributions for all transitions calculated so far.

The theoretical cross section $\sigma(\mathrm{El})$ for the electric transition at 162 MeV is similar to that given by the experimental data but is smaller by about a factor $\frac{1}{2}$ in absolute value. The isotropic term in the dipole approximation has the smallest value for this kind of calculation[23]; it is possible to make it larger by taking into account the final-state interactions.[6] As the other transitions are successively taken into account, a trend toward good agreement with the experimental data is obtained at 162 MeV. But this trend in the angular distributions does not hold at higher energies. The theoretical peaks in the angular distributions shift to zero angle. Also, the total cross sections are as much as four times the experimental values. The excitation curves in Fig. 4 show the total cross sections for all transitions, as well as the cross sections for the electric transitions alone.

IV. DISCUSSIONS OF THE RESULTS

We now have the effects of the various transitions (neglecting the effects of the virtual meson exchange current). The energy dependence of the total cross sections, as can be seen from Fig. 4, gives values larger than the experimental values in the region of photon energy higher than 400 MeV. The comparison with experiment at these high energies is not very significant, however, and it is tempting to say that the cross sections can be accounted for by the electric transitions alone. However, the total magnetic contributions do appear to contribute as much as twice the electric ones on the basis of our calculations. Let us look at our approximations to see whether the magnetic transitions should really give big contributions of this order.

Looking back to the radial integrals (12) and (19), we shall estimate the errors due to our choice of deuteron wave functions (4) and (5), namely, the effects of the disregard of the hard core[24] (assuming a hard-core radius $r_0=0.2$). The estimations of the errors in the dipole approximation for $I(Fd)$, $I(Pd)$, and $I(Ps)$ are 10^{-3},

[23] In a previous calculation (reference 11) the author obtained 79 μb at a photon energy of 80 MeV. This value is about 10% smaller than the theoretical value obtained when final-state interaction is taken into account.

[24] Calculations taking into account the hard core are being done and will be published later.

0.07, and 1.8% at the energy 162 MeV, and 0.15, 4.3, and 50% at the energy 833 MeV. The fact that the error in $I(Ps)$ increases from 1.8% at 162 MeV up to 50% at 833 MeV means that the integral for $I(Ps)$ must be canceled in the region $x \gtrsim 1$, but is not changed in the region $x \lesssim 1$, and everywhere decreases to smaller values with higher energies. The contributions of $I(Ps)$ to the cross section are fortunately very small (i.e., 0.67% of 2.6% in this energy region).

The contributions in the region $x \lesssim 1$ to the radial integrals (12) are, as can easily be seen, smaller than for the magnetic transitions (19). For the radial integrals of the spin magnetic transition (19) especially, the transition amplitude from the deuteron s state to the final s state results in a very big contribution in the region $x \lesssim 1$, because a major part of the final s-state wave function $j_0(kx)$ is concentrated within this region and the estimated error already amounts to 38% at 162 MeV. This circumstance and the importance of the $Z_{s(t)}$ term in Eqs. (16) and (17) make the cross sections large. Moreover, the effect of the hard core on the final states makes the values of the overlap integrals quite small. For this reason, we are tempted to conclude that the large contribution of the magnetic transitions to the amount of the total cross sections depends, at least in part, upon the nature of our approximations, namely, the disregard of the effects of the hard core on the deuteron wave function and on the final-state wave function.

In the present calculations, the final-state interactions are not considered at all, so that the polarization of the outgoing particles cannot be obtained. The effect of the higher electric multipole transitions and of their retardations is to shift the angular distributions forward, but not to increase the total cross sections very much. The forward shifts of the angular distributions is emphasized by the interference terms between the electric and magnetic transitions. Hence, it may be noted that the polarizations—assuming they were to be calculated by means of this approximation—would appear very small for forward, but very large and with opposite sign for backward directions, consistent with the calculations of Rustgi *et al.*[4]

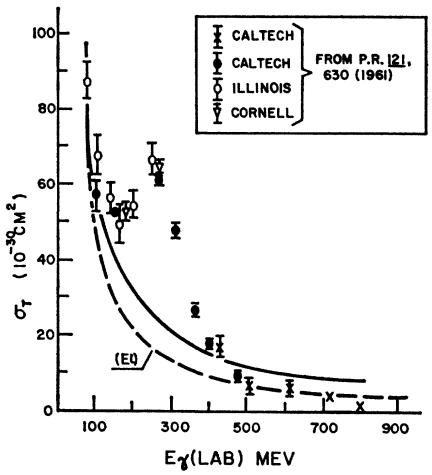

FIG. 4. Variation of the total cross section (solid line) and of the cross section for the electric transitions only (dashed line) with incident photon energy.

ACKNOWLEDGMENTS

The author would like to express his sincere thanks to Professor L. E. H. Trainor, for discussions and for help in preparing the manuscript. The author also appreciates the assistance given by Mrs. F. Mather with the numerical calculations by means of an IBM-1620 electric computer. Support of this research by the National Research Council of Canada is gratefully acknowledged.